SYNTHESIS AND CHARACTERIZATION OF HYDROXYAPATITE

Thesis Submitted in Partial fulfilment of the requirement for

The award of the degree of

Master of Technology (M.Tech.)

In

MATERIALS AND METALLURGICAL ENGINEERING

Submitted by

RAMANDEEP SINGH
ROLL No. 601002003

Under the guidance
of
Dr. KULVIR SINGH
Associate Professor and Head

(School of Physics and Materials Science)

School of Physics and Materials Science
Thapar University, Patiala
Patiala (Punjab)-147004

June-2012

Dedicated to My Parents

CERTIFICATE

This is to certify that the thesis entitled "**Synthesis and Characterization of Hydroxyapatite**" submitted by **Mr. Ramandeep Singh**, Roll No. **601002003** in the partial fulfilment of the requirement for the award of the degree of **Mater of Technology** in Materials and Metallurgical Engineering from the School of Physics and Materials Science, **Thapar University, Patiala**, is record of candidate's own work carried out by him under my supervision and guidance. The matter embodied in this report has not been submitted in part or full to any other university or institute for the award of any degree.

Dr. Kulvir Singh

Supervisor

(Associate Professor and Head)

School of Physics and Materials Science

Thapar University, Patiala

Countersigned by:

Dr. Kulvir Singh

(Associate Professor and Head)

School of Physics and Materials Science

Thapar University, Patiala

Punjab

Dr. S.K. Mohapatra

(Dean, Academic Affairs)

Thapar University, Patiala

Punjab

ACKNOWLEDGEMENT

First of all I would like to extend my gratitude towards my supervisor, **Dr. Kulvir Singh** (Associate Professor and Head), School of Physics and Materials Science, Thapar University, Patiala, for giving me a chance to work in his supervision and without his help and constant guidance this thesis would have not completed.

I would also like to thank **Dr. O.P. Pandey**, Sr. Professor, School of Physics and Materials Science for his constant guidance and encouragement. He has been very helpful in improving my dissertation. I am grateful to him for sharing his time and expertise. His comments and views were very insightful and helpful.

I wish my sincere thanks to **Dr. Bhupendrakumar Chudasama** (Assistant Professor) and **Dr. Puneet Sharma** (Assistant Professor), School of Physics and Materials Science, who always took keen interest in guiding me during my work.

I am also grateful to **Mrs. Nidhi Andhariya**, PDF Scholar, School of Physics and Materials Science for her encouragement and execution of report work and providing me invaluable support and training in various techniques and uses of equipment.

My special thanks to *PG Lab Incharge* **Mr. Purushottam Kumar** carrying out the SEM analysis required for my work during the thesis and **Mr. Jant Singh**, for his all kind of help in PG Lab for creating a healthy research environment

I would also like to thank **Mr. Jagtar Singh**, (Sophisticated Analysis and Instrument Centre, Panjab University, Chandigarh) for carrying out the X-ray diffraction needed for my work.

I would like to give my special thanks to Research Scholars Samita Thakur, Chandni Bansal and Gaurav Singla for helping me at various stages of my experimental work.

Ramandeep Singh

(Ramandeep Singh)

Roll No. 601002003

INDEX

List of Symbols and Abbreviations

HA	Hydroxyapatite
CP	Calcium Phosphate
MPa	Mega Pascal
GPa	Giga Pascal
μm	Micrometer
TCP	Tri Calcium Phosphate
TPS	Titanium Plasma Spray
XRD	X-ray Diffraction
TGA	Thermogravimetric Analysis
DTA	Differential Thermal Analysis
rpm	Revolutions Per Minute
SEM	Scanning Electron Microscopy
g	Grams
EDS	Energy Dispersive Spectroscopy
nm	Nanometer

List of Figures

List of Tables

ABSTRACT

Hydroxyapatite (HA) is successfully used as a bioimplant material because it resembles the bone apatite up to a great extent and possesses good biocompatibility. In the present study, HA powder has been synthesized by sol-gel technique. The as prepared powder was sintered at two different temperatures 400°C and 750°C to increase its crystallinity. A HA-CNT composite sample was also prepared to compare the results. The final sintered powder was characterized by X-ray diffraction analysis, Scanning Electron Microscopy (SEM) to know about its phase content and morphology. Thermal Analysis (TGA-DTA) was carried out to study the stability of the powder with respect to temperature. Energy Dispersive Spectroscopy (EDS) was carried out to get the information about the elements present in the final powder and their respective weight percentage. The XRD pattern indicated the formation of $Ca_5HO_{13}P_3$ and $Ca_2H_8O_{11}P_2$ phases. The higher temperature sintering of the as prepared samples leads to the good crystallinity. On the other hand, the powder sintered at 400°C could not show any crystalline phase formation. Moreover, the addition of CNTs increased the crystallinity and crystallite size of the powder.

CHAPTER 1

INTRODUCTION

1.1 Biomaterials

Biomaterial is a material that can be used and adapted for a medical application. Biomaterials can have a benign function, such as being used for a heart valve, or may be bioactive; used for a more interactive purpose such as hydroxyapatite coated hip implants. Biomaterials are also used every day in dental applications, surgery, and drug delivery.

While a definition for the term 'biomaterial' has been difficult to formulate, more widely accepted working definition may be given as: "A biomaterial is any material, natural or man-made, that comprises whole or part of a living structure or biomedical device which performs, augments, or replaces a natural function"[1].

During recent decades, the ageing population and some other reasons have led to a surge of bone-related diseases and bone fractures, which must be treated. However, in order to be accepted by the living body, all implantable items must be prepared from a special class of materials i.e. the above mentioned biocompatible materials or simply biomaterials. These biomaterials belong to all 5 major classes of materials: metals, ceramics, polymers, composites and natural materials. Wide range of these materials used in medical field is a result of materials research done in the last 50 years by controlling the composition, purity, physical properties of the materials and synthesizing new materials with new and special properties. These biomaterials are modified according to the needs of medical devices such as woven polymer fibers in vascular grafts, bundles of cellulose acetate fibers in artificial kidney dialyses and titanium alloys in hip replacements [2].

The common property of all the biomaterials is biocompatibility or non-toxicity which defines the feature of a material that is not recognized by the body as a potentially harmful foreign substance [2]. Not all biocompatible materials are inert in the body but the highly bioactive ones incorporate to the actions of body like providing a host matrix for tissue growth or being slowly replaced by the growing tissue. Biocompatible materials are categorized as bioinert, resorbable and bioactive based on tissue response. Bioinert materials induce formation of a fibrous tissue of

variable thickness, interfacial bond forms on bioactive materials and resorbable materials are replaced by the surrounding tissue [2].

1.2 Classification of Biomaterials

Synthetic materials currently used for biomedical applications include metals and alloys, polymers, and ceramics. Because the structures of these materials differ, they have different properties and, therefore, different uses in the human body.

1.2.1 Metallic Biomaterials

Metals have been used almost completely for load-bearing implants, like hip and knee prostheses and fracture fixation wires, pins, screws, and plates. Metals have also been used as parts of artificial heart valves, as vascular stents, and as pacemaker leads. Although pure metals are sometimes used, alloys often provide better mechanical properties, such as strength and corrosion resistance. Three material groups are mostly used as biomedical metals: 316L stainless steel, cobalt-chromium-molybdenum alloy and pure titanium and titanium alloys [3]. The main points to be keep in mind while selecting metals and alloys for biomedical applications are biocompatibility, appropriate mechanical properties, corrosion resistance and reasonable cost.

In metals, the loose, nondirectional electron bonding allows the atoms/ions to be parted more easily. Consequently, although their mechanical properties make metals the appropriate choice for many biomedical applications, susceptibility to chemical degradation is an aspect that must be considered. The mechanical properties of materials play an important role when designing load-bearing orthopedic and dental implants. With a few exceptions, the high tensile and fatigue strength of metals, compared with ceramics and polymers, make them the materials of choice for implants that carry mechanical loads [3].

1.2.2 Polymeric Biomaterials

Polymers are the most widely used materials in biomedical applications. They are the appropriate choice for cardiovascular devices as well as for replacement and growth of various soft tissues [3]. Polymers also are used in drug delivery systems, in diagnostic aids and as a scaffolding material for tissue engineering applications. For example, currently, these are used in vascular grafts, heart valves, artificial hearts, breast implants, contact lenses, intraocular lenses, components of extracorporeal oxygenators, dialyzers and plasmapheresis units, coatings for

pharmaceutical tablets and capsules, sutures, adhesives, and blood substitutes [3]. The mechanical properties of polymers depend on several factors, including the composition and structure of the macromolecular chains and their molecular weight. Polymers have much lower strengths and moduli as compared to metals and ceramics, but they can be deformed to a greater extent before failure. So, polymers are generally not used in biomedical applications that bear loads e.g. body weight.

1.2.3 Ceramic and Glass Biomaterials

Ceramics and glasses are used as components of hip implants, dental implants, middle ear implants and heart valves. Overall, however, these biomaterials have been used less extensively than either metals or polymers. Some of the most promising biomaterials in this category are bioceramics such as hydroxyapatite (HA), calcium phosphates, bioactive glasses and related composite materials combining bioactive inorganic materials with biodegradable polymers [3]. The major drawbacks to the use of ceramics and glasses as implants are their brittleness and poor tensile properties. Although they can possess good strength when loaded in compression, ceramics and glasses fail at low stress when loaded in tension or bending. Among bioceramics, alumina has the maximum mechanical properties, but its tensile properties are still lesser than metallic biomaterials. But it has low coefficient of friction and wear rate, so it is generally used as a bearing surface in joint replacements.

The mechanical properties of calcium phosphates and bioactive glasses make them inappropriate as load-bearing implants. Clinically, hydroxyapatite has been used as filler for bone defects and as an implant in load-free anatomic sites (for example, nasal septal bone and middle ear) and as a coating on metallic orthopedic and dental implants to promote their fixation in bone [3].

1.3 Bioceramics

Ceramics used for the repair and reconstruction of diseased or damaged parts of the musculo-skeletal system, are termed bioceramics. In the late 1960s, much interest was raised towards the biomedical applications of various ceramic materials. These are the materials which are biocompatible. Bioceramics has become one of the major fields in biomaterials. Many different bioceramics, with various material compositions and characteristics producing different biological behaviour, result in a wide range of medical applications. Oxides are the most

commonly used ceramics and these are also available in large quantities in nature. The chemical synthesis, shaping and heat treatment processes of oxides are relatively simple compared to other materials [2].

1.4 Types of Bioceramics

Ceramic materials are made of an inorganic non-metallic oxide. Bioceramics can be produced in crystalline and amorphous forms, and they are generally classified according to their chemical compositions into two groups; calcium phosphates (CP) and others, including yttria (Y_2O_3)-stabilized tetragonal zirconia (ZrO_2) (YTZP), alumina (Al_2O_3) and some silicate and phosphate families of glasses and crystallized glasses (glass-ceramics). Depending on their *in vivo* behaviour, ceramics are classified as bioinert, bioresorbable or bioactive.

1.4.1 Bioinert Bioceramics

Bioinertness means that no chemical interaction takes place between the implant material and host tissue. So biologically inert, or bioinert materials are those which do not start a response or interact when introduced to biological tissue. In other words, introducing the material to the body will not cause a reaction with the host. Bioinert materials were developed because the degradation products of previously used materials such as metal implants, glass ceramics, alloys, and polymers were a fear dur to their toxic nature. The degradation products of these materials are often toxic, causing an allergenic or carcinogenic response. In starting these materials were used for vascular surgery due to the need for surfaces, which do not cause clotting of the blood. Although biocompatibility was enhanced by the growth of bioinert materials, the absence of a chemical interaction between materials and host tissue is a disadvantage of these materials. The incorporation and integration is disturbed and a fibrous tissue layer surrounding the implant is formed, especially in weight bearing applications [4].

1.4.2 Bioactive Bioceramics

The integration of biomaterials was significantly improved by the introduction of bioactive substances. Bioactivity is the ability of the material to directly ‘bond’ to bone through chemical interaction and not physical or mechanical attachment. Bioactivity has been characterized *in vitro* and *in vivo* as the ability of the material to form carbonate apatite (similar to bone apatite)

on its surface [2]. This occurs through a time – dependent kinetic modification of the surface, triggered by their implantation within the living bone. An ion – exchange reaction between the bioactive implant and surrounding body fluids results in the formation of a biologically active carbonate apatite layer on the implant that is chemically and crystallographically equivalent to the mineral phase in bone. It has been learnt that this interaction consists mainly of the formation of a layer of hydroxyapatite on the surface, whereas the bulk of the material remains unchanged. This layer of hydroxyapatite increases integration and incorporation of biomaterials [4].

1.4.3 Bioresorbable Bioceramics

Bioresorption is a biological mechanism by which certain ceramic materials resorb partially or completely and thereby disappear partially or completely over a period of time. So bioresorbable refers to a material that starts to dissolve (resorbed) when placed within the human body and slowly replaced by advancing tissue (such as bone) [5]. Ideally, the rate of resorption, resulting in a sequentially changing bone-biomaterial interface, should be same to the rate of formation of new bone. Almost all bioresorbable ceramics are variations of calcium phosphate. The advantages of a resorbing material are clear. First of all, no foreign body remains in place during the rest of the lifetime. Second, remodeling of the newly formed bone is not influenced by the presence of the ceramic. Third, after resorption of the ceramic material the remodeled bone is stronger than the combination of a ceramic and newly formed bone [4]. According to their activities various bioceramics can be classified as given in table 1.1.

Table 1.1: Different bioceramics and their types.

Ceramic	Chemical Formula	Type
Alumina	Al_2O_3	Bioinert
Zirconia	ZrO_2	Bioinert
Bioglass	$Na_2OCaOP_2O_3SiO$	Bioactive
Hydroxyapatite	$Ca_{10}(PO_4)_6(OH)_2$	Bioactive
Tricalcium Phosphate	$Ca_3(PO_4)_2$	Bioresorbable

1.4.3.1 Alumina (Al_2O_3)

Corundum known as α-alumina is the alumina ceramic used for biomedical application. Al_2O_3 molecule is one of the most stable oxides because of high energetic ionic and covalent bonds between Al and O atoms. These strong bonds leave the ceramic unaffected by galvanic reactions. Adverse conditions such as strong acidic or alkaline environment at high temperatures do not damage alumina properties. Under compression alumina shows good resistance but under tensile condition it shows brittleness. At room temperature alumina does not show plastic deformation before fracture and once started fractures progress very rapidly (low toughness). Tensile strength of alumina improves with higher density and smaller grain size [6]. An alumina ceramic shows the characteristics of high hardness and high abrasion resistance. The reasons for the excellent wear and friction behavior of Al_2O_3 are associated with the surface energy and surface smoothness of this ceramic. There is only one thermodynamically stable phase, i.e. Al_2O_3 that has a hexagonal structure with aluminium ions at the octahedral interstitial sites [7]. Generally alumina is used for knee prostheses, bone and dental screws, alveolar ridge and maxillofacial reconstruction, ossicular bone substitutes, corneal replacements and segmental bone replacements.

Table 1.2 Mechanical properties of biomedical grade alumina.

Density	3.97 g/cm3 (99.9% Al_2O_3)
Hardness	2200 Vickers
Bend Strength	500 MPa
Compressive Strength	4100 MPa
Fracture Toughness	4 $MPa/m^{1/2}$
Young's Modulus	380 GPa
Thermal Coefficient of Expansion	$8x10^{-6}$ 1/K

1.4.3.2 Zirconia (ZrO_2)

Zirconia is an inert ceramic in its pure form which possesses extraordinary properties when doped with certain stabilizing oxides such as yttria, magnesia and calcia. It is a well-known polymorph that occurs in three forms: monoclinic (M), tetragonal (T), and cubic (C). Pure zirconia is monoclinic at room temperature. This phase is stable up to 1170°C. Above this temperature it transforms into tetragonal and then into cubic phase at 2370°C. During cooling, a T to M transformation takes place in a temperature range of about 100°C below 1070°C. The improved mechanical properties due to transformation toughening of tetragonal zirconia are utilized in biocomposites as well as conventional ceramic applications because of its good biocompatibility [2]. Zirconia is a biomaterial that has good applications due to its high mechanical strength and fracture toughness. Zirconia ceramics have several advantages over other ceramic materials due to the transformation toughening mechanisms operating in their microstructure that can be manifested in components made out of them [7]. To stabilize zirconium oxide a little amount of non-metallic oxide such as MgO, CaO and Y_2O_3 are added. The type and amount of additives to stabilize zirconia in its tetragonal crystal structure is the important variable in composition that affects all of the mechanical properties. The yttria content is the most significant controlling variable in yttria stabilized zirconia ceramics. In order to improve the mechanical properties it is important to have a microstructure free of any monoclinic phase which would act as a flaw and this dictates the minimum level of stabiliser added. Tetragonal zirconia experiences degradation when in contact with water at temperatures in the

range of 200-300 °C due to ageing of the metastable phase which restricts its use in long term applications. Biomedical grade zirconia exhibits the best mechanical properties of oxide ceramics. The general biomedical applications of zirconia are THR (total hip replacement) ball heads, THR acetabular inlays, THR condyles, Finger joints, Spinal spacers, humeral epiphysis and hip endoprostheses [6].

Table 1.3 Mechanical properties of zirconia.

Density	6.05 g/cm^3
Hardness	1200 HV
Bend Strength	900-1200 MPa
Compressive Strength	2000 MPa
Fracture Toughness	7-10 $MPa/m^{1/2}$
Young's Modulus	210 GPa
Thermal Coefficient of Expansion	$11x10^{-6}$ 1/K

1.4.3.3 Bioglass

Bioglasses are interesting and versatile class of materials. Structurally all silica-based glasses have the same basic building block - SiO_4^{4-}. Glasses of various compositions can be obtained and they show very different properties [7]. The base components in most bioactive glasses and glass-ceramics, made by traditional high temperature melting, casting and sintering, are SiO_2, Na_2O, CaO and P_2O_5. These bioglasses are embedded in a biomaterial support to form prosthetics for hard tissues. Such prosthetics are biocompatible, show excellent mechanical properties and are useful for orthopedic and dental prosthetics. The bioactive glasses can be produced with the conventional technologies of glass industry, but it is necessary to verify the purity of the raw materials to avoid the contamination by impurities and loss of volatile elements like Na_2O or P_2O_5. Bioactive glasses are soft in nature and therefore final shape can be given with conventional tools. The bioactive glasses can be used to repair and rebuild damaged tissues, specifically hard tissues. Bioactive glasses are generally divided into two groups: class A and class B. Class 'A' bioglasses are osteoproductive in nature. These can bond to soft and hard tissues. They releases silica ions in the form of silicic acid and provide a silica gel layer which

further enhancesthe amorphous CaP layer and rapidly crystallizes hydroxyapatite layer. Bioglass 45S5 which contains 45% SiO_2 wt%, 24.5% Na_2O wt%, 24.5% CaO wt% and 6% P_20_5 wt% is a class 'A' bioglass. Class 'B' bioactive bioglasses are osteoconductive in nature. They do not produce silica gel layer and they bond to hard tissues only [8]. The main clinical applications of bioactive bioglasses are coatings for chemical bonding (for orthopedic, dental, and maxillofacial prosthetics), dental implants, alveolar ridge augmentations, otolaryngological, maxillofacial reconstruction, percutaneous access devices [9].

1.5 Hydroxyapatite

Hydroxyapatite is the calcium phosphate complex which is the main mineral of bones. It is the crystallized form of calcium orthophosphate hydroxide, with chemical formula $Ca_{10}(PO_4)_6(OH)_2$, virtually insoluble in water and in many aqueous solvents. It occurs as a mineral in phosphate rock. It is the principal inorganic constituent of bone matrix and teeth, which imparts rigidity to these structures, and consists of hydrated calcium phosphate. Chemically prepared hydroxyapatite is useful in the separation of proteins or nucleic acids by adsorption chromatography. It is used in orthopedic and dental prostheses and in the prevention of osteoporosis (a disease of bones that leads to an increased risk of fracture). Unlike the other calcium phosphates, hydroxyapatite does not break down under physiological conditions. In fact, it is thermodynamically stable at physiological pH and actively takes part in bone bonding, forming strong chemical bonds with surrounding bone. This property has been exploited for rapid bone repair after major trauma or surgery. Hydroxyapatite (HA) is a biologically active calcium phosphate ceramic that is used in surgery to replace and mimic bone. While HA's bioactivity means it has a significant ability to promote bone growth along its surface, its mechanical properties are insufficient for major load bearing devices [10]. The mineral component in the living bone is also a hydroxyapatite, the so-called biological apatite. The amount of the biological apatite in bone is approximately 70% by weight. It is believed that synthetic hydroxyapatite used for bone replacement would be entirely compatible with the body. When exposed to body fluids, hydroxyapatite will bond to bone by forming indistinguishable unions. The bonding starts by formation of carbonate-apatite crystals on the bone, thus promoting the adhesion of matrix-producing cells and organic molecules as a result of surface chemistry and surface charges. Biological apatite, which comprises the mineral phase of human

bone, is usually referred to as hydroxyapatite. Actually, biological apatite differs from pure hydroxyapatite, and it is more appropriate to refer to as carbonate apatite. Biological apatite contains ions such as Na^+, K^+, Mg^{2+}, F^- and Cl^- in solid solution. Some of the PO_4^{3-} may also be replaced by CO_3^{2-}. Thus, the ideal Ca/P molar ratio of pure hydroxyapatite (1.67) differs slightly from that of biological apatite (1.72-1.80) [11].

1.6 Properties of Hydroxyapatite

1.6.1 Mechanical Properties

The most important property or feature of the hydroxyapatite is its chemical similarity with the mineralized bone of human tissue, synthetic HA exhibits strong affinity to bone hard tissue. Formation of chemical bond with the host tissue offers HA a greater advantage in clinical applications than most other bone substitutes [12]. From the mechanical point of view, calcium orthophosphate bioceramics appear to be brittle polycrystalline materials for which the mechanical properties are governed by crystallinity, grain size, grain boundaries, porosity and composition. It appears to be very sensitive to slow crack growth. For dense bioceramics, the strength is a function of the grain size. Finer grain size materials have smaller flaws at the grain boundaries and thus are stronger than bioceramics with larger grain sizes. In general, the mechanical properties decrease significantly with increasing content of an amorphous phase, microporosity and grain size, while a high crystallinity, a low porosity and small grain size tend to give a higher stiffness, a higher compressive and tensile strength and a greater fracture toughness. Thus, calcium orthophosphate bioceramics possess poor mechanical properties (for instance, a low impact and fracture resistances) that do not allow to use them in load-bearing areas, such as artificial teeth or bones. For example, fracture toughness of HA bioceramics does not exceed ~1.2 $MPa \cdot m^{1/2}$ (human bone: 2–12 $MPa \cdot m^{1/2}$). It decreases almost linearly with increasing porosity. Generally, fracture toughness increases with decreasing grain size. However, in some materials, especially non-cubic ceramics, fracture toughness reaches the maximum and rapidly drops with decreasing grain size. For example, when the fracture toughness of pure hot pressed HA was investigated with grain sizes of 0.2–1.2 μm, There appeared to be two distinct trends, where fracture toughness decreased with increasing grain size above ~0.4 μm and subsequently decreased with decreasing grain size. The maximum fracture toughness measured was 1.20 ± 0.05 $MPa \cdot m^{1/2}$ at ~0.4 μm. Fracture energy of HA bioceramics is in the range of 2.3–

20 J/m^2, while the Weibull modulus is low (~5–12) in wet environments, which means that HA behaves as a typical brittle ceramics and indicates low reliability of HA implants [12].

Bending, compressive and tensile strengths of dense HA bioceramics are in the range of 38–250 MPa, 120–900 MPa and 38–300 MPa, respectively. Similar values for porous HA bioceramics are in the range of 2–11 MPa, 2–100 MPa and ~3 MPa, respectively [12]. These wide variations in the properties are due to both structural variations (e.g., an influence of remaining microporosity, grain sizes, presence of impurities, *etc*.) and manufacturing processes, as well as caused by a statistical nature of the strength distribution. Strength has been found to increase with increasing Ca/P ratio and it can reach a maximum value around Ca/P ~1.67 (stoichiometric HA) and it decreases suddenly when Ca/P > 1.67. Furthermore, strength decreases almost exponentially with increasing porosity. However, by changing the pore geometry, it is possible to control the strength of porous bioceramics. It is also interesting to note that porous HA bioceramics are considerably less fatigue resistant than dense ones. Both grain sizes and porosity influence the fracture path, which itself has little effect on the fracture toughness of calcium orthophosphate bioceramics [12].

Young's (or elastic) modulus of dense HA bioceramics is in the range of 35–120 GPa, which is more or less similar to those of the most resistant components of the natural calcified tissues (dental enamel: ~74 GPa, dentine: ~21 GPa, compact bone: ~18–22 GPa) [12]. Nevertheless, dense bulk compacts of HA have mechanical resistances of the order of 100 MPa versus ~300 MPa of human bones, diminishing drastically their resistance in the case of porous bulk compact. Young's modulus measured in bending for HA lies between 44 and 88 GPa. Recently, a considerable anisotropy in the stress-strain behavior of the perfect HA crystals were found. The crystals appeared to be brittle for tension along the *z*-axis with the maximum stress of ~9.6 GPa at 10% strain. Vickers hardness of dense HA bioceramics is within 3–7 GPa, while the Poisson's ratio for the synthetic HA is about 0.27, which is close to that of bones (~0.3) [12]. At temperatures within 1000–1100°C, dense HA bioceramics has been found to exhibit superplasticity with a deformation mechanism based on grain boundary sliding. Furthermore, both the wear resistance and friction coefficient of dense HA bioceramics are comparable to those of dental enamel [12].

In order to improve the reliability of calcium orthophosphate bioceramics, diverse reinforcements (ceramics, metals or polymers) have been applied to manufacture various biocomposites and hybrid biomaterials [12].

1.6.2 Electrical Properties

Sometimes, electrical properties of calcium orthophosphate bioceramics are also studied. For example, a surface ionic conductivity of both porous and dense HA bioceramics has been examined for humidity sensor applications, since the room temperature conductivity is influenced by relative humidity. The ionic conductivity of HA has been a subject of research for its possible use as a sensor to alcohol, carbon dioxide or carbon monoxide gas. Electrical measurements have also been used as a characterization tool to study the evolution of microstructure in HA [12]. Interestingly, the electrical properties of calcium orthophosphate appear to influence their biomedical applications. For example, there is an interest in polarization of HA to generate a surface charge by the application of electric fields at elevated temperatures [12]. The presence of surface charges on HA has shown to have a significant effect on both *in vitro* and *in vivo* crystallization of biological apatite. Moreover, growth of both biomimetic calcium orthophosphates and bones was found to be accelerated on negatively charged surfaces and decelerated on positively charged surfaces. The dielectric properties of hydroxyapatite has been examined to understand the decomposition of HA to tri-calcium phosphate (TCP) ($Ca_3(PO_4)_2$ as a result of the dehydration of hydroxyl ions at elevated temperatures since TCP is thought to have higher bioactivity than HA, but is also more biodegradable [12].

1.6.3 Possible Transparency

Single crystals of all calcium orthophosphates are optically transparent for visible light [12]. As bioceramics of calcium orthophosphates have a polycrystalline nature with a random orientation of big amounts of small crystals they are opaque and of white color, unless colored dopants have been added. However, in some cases, transparency is convenient to provide some essential advantages (e.g., to enable direct viewing of living cells in a transmitted light). Thus, sometimes transparent calcium orthophosphate bioceramics are prepared.

1.6.4 Bioactivity

Bioactivity is the ability of the material to directly 'bond' to bone through chemical interaction and not physical or mechanical attachment. Bioactivity has been characterized *in vitro* and *in vivo* as the ability of the material to form carbonate apatite (similar to bone apatite) on its surface [13].

1.6.5 Osteoconductive property

Bioactive materials (calcium phosphates and bioactive glasses) also have osteoconductive properties – an ability to serve as a scaffold or template to guide the newly forming bone along its surfaces. Osteoconductive materials allow bone cell attachment, proliferation, migration and phenotypic expression, leading to formation of new bone in direct apposition to the biomaterial, thus creating a uniquely strong interface [13].

1.6.6 Porosity

Porosity is defined as the percentage of void spaces in solids and it is a morphological property independent of the material. The surface area of porous bodies is much higher, which guarantees a good mechanical fixation in addition to providing sites on the surface that allow chemical bonding between the bioceramics and bones [12]. Furthermore, a porous material may have both closed (isolated) pores and open (connected) pores. Connected pores look like tunnels and are accessible by gases, liquids and particulate suspensions. Moreover, dimensions of open pores are directly related to bone formation, since such pores grant both the surface and space for cell adhesion along with bone growth. On the other hand, pore interconnection provides the way for cell distribution and migration. Namely, porous HA bioceramics can be colonized by bone tissues. Therefore, interconnecting macro porosity (pore size >100 μm), which is defined by its capacity to be colonized by cells, is intentionally introduced in solid bioceramics (Figure 1.1). Macro porosity is usually formed due to a release of various volatile materials and, for that reason, incorporation of pore-creating additives (porogens) is the most popular technique to create macroporosity. The porogens are crystals or particles of either volatile (they evolve gases at elevated temperatures) or soluble substances, such as paraffin, naphthalene, sucrose, $NaHCO_3$, gelatin, polymethylmethacrylate or even hydrogen peroxide [12].

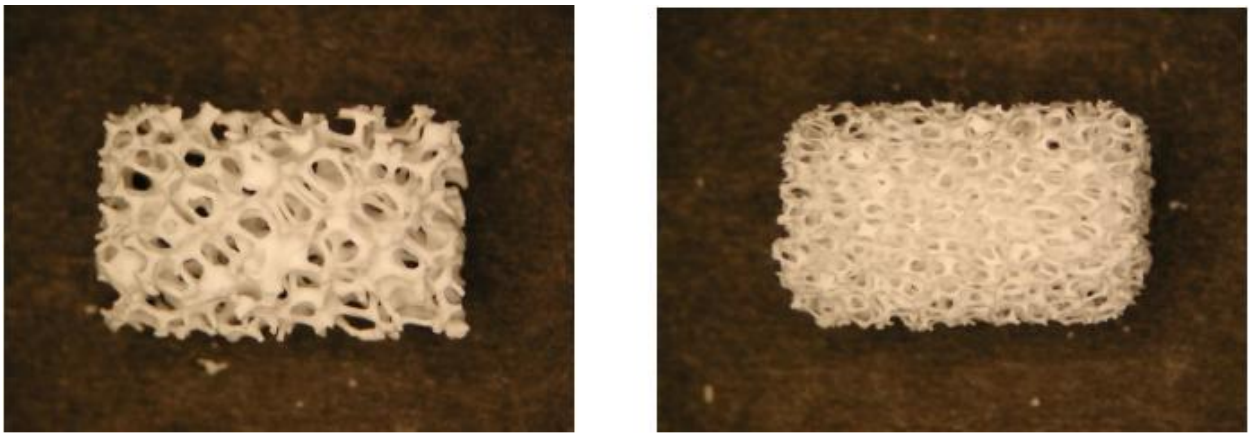

Figure 1.1 Photographs of a commercially available porous calcium orthophosphate bioceramic with different porosity.

Briefly the key properties of the HA can be mentioned as follows [14]:

- The ability to integrate in bone structures and support bone ingrowth, without breaking down or dissolving (i.e. it is bioactive).
- Generally speaking dense hydroxyapatite does not have the mechanical strength to enable it to succeed in long term load bearing applications.

1.7 Applications of Hydroxyapatite

Due to high brittleness (associated to a low crack resistance), biomedical applications of calcium orthophosphate bioceramics are focused on production of non-load bearing implants, such as pieces for middle ear surgery, filling of bone defects in oral or orthopedic surgery, as well as coating of dental implants and metallic prosthesis.

Applications include dental implants, percutaneous devices and use in periodontal treatment, healing of bone defects, fracture treatment, total joint replacement (bone augmentation), orthopedics, cranio-maxillofacial reconstruction, otolaryngology and spinal surgery. Depending upon the required properties, different calcium orthophosphates might be used. For example, Figure 1.2 shows some randomly chosen samples of the commercially available calcium orthophosphate bioceramics for bone graft applications.

Generally HA can be used in the following forms:

1.7.1 Implant Coatings

Coatings of hydroxyapatite are often applied to metallic implants (most commonly titanium/titanium alloys and stainless steels) to alter the surface properties of the materials. In this manner the body sees hydroxyapatite-type material to which it accepts without any problem. Without the coating the body would see a foreign body and work in such a way as to isolate it from surrounding tissues. At present, the only commercially accepted method of applying hydroxyapatite coatings to metallic implants is plasma spraying [14].

1.7.2 Bone Fillers

Hydroxyapatite may be employed in forms such as powders, porous blocks or beads to fill bone defects or voids. These may arise when large sections of bone have had to be removed (e.g. bone cancers) or when bone augmentations are required (e.g. maxillofacial reconstructions or dental applications). The bone filler will provide a scaffold and encourage the rapid filling of the void by naturally forming bone and provides an alternative to bone grafts. It will also become part of the bone structure and will reduce healing times compared to the situation, if no bone filler was used [14].

1.7.3 HA as Abrasive

A rough surface of Ti or Ti alloy implant was reported to promote greater osteointegration reflected by stronger bone-implant interface. Implant surface roughening accomplished by grit-blasting with abrasives, usually silica or alumina. More recently HA or apatite abrasive (biphasic calcium phosphate) has gained popularity as the abrasive of choice for orthopedic and dental. Implant surface grit-blasted with HA or apatite abrasive appears to be cleaner (free of inclusions) compared with alumina and appear to promote higher bone contact [13].

CHAPTER 2

LITERATURE REVIEW

2.1 Historical Background

The performance of living tissues is the result of millions of years of evolution, while the performance of acceptable artificial substitutions that humankind has designed to repair damaged tissues are only a few decades old. However, attempts to repair the human body with the use of implant materials are recorded in the early medical writings of the Hindu, Egyptian and Greek civilizations. The earliest successful implants were in the skeletal system. Historically, selection of the materials was based on their availability and the skill of the individual making and applying the prosthetic. Archaeological findings exhibited in museums showed that materials used to replace missing human bones and teeth included animal or human (from corpses) bones and teeth, shells, corals, ivory (elephant tusk), wood, as well as some metals (gold or silver). For instance, the Etruscans learned to substitute missing teeth with bridges made from artificial teeth engraved from the bones of oxen, while in ancient Phoenicia loose teeth were bound together with gold wires, tying artificial ones to neighboring teeth.

The first widely tested artificial bioceramic was plaster of Paris. However, in the past, many implantations failed due to infections, which tended to be exacerbated in the presence of implants, since they provided a region inaccessible to the body's immunologically competent cells. Thus, the use of biomaterials did not become practical until the advent of an aseptic surgical technique developed by Lister in the 1860s. Furthermore, there was a lack of knowledge about the toxicity of selected materials. In this frame, application of calcium orthophosphates appears to be logical due to their similarity with the mineral phases of bones and teeth. Calcium orthophosphates are not toxic and do not cause cell death in the surrounding tissues. However, according to available literature, the first attempt to use them (it was TCP *i.e.* tricalciuam phosphate) as an artificial material to repair surgically created defects in rabbits was performed in 1920 [12]. The second clinical report was published 30 years later. More than 20 years afterwards, the first dental application of a calcium orthophosphate in surgically created periodontal defects and the use of dense HA cylinders for immediate tooth root replacement were reported. On April 26, 1988, the first international symposium on bioceramics was held in Kyoto, Japan [12].

Commercialization of the dental and surgical applications of calcium orthophosphate (mainly, HA) bioceramics occurred in the 1980s, largely due to the pioneering efforts by Jarcho in the USA, De Groot in Europe and Aoki in Japan. Shortly afterwards, HA became a bioceramic of reference in the field of calcium orthophosphates for biomedical applications. Preparation and biomedical applications of apatites derived from sea corals (coralline HA) and bovine bone were reported at the same time [12].

2.2 Recent developments in bioceramics

Best *et al.* [15] published their report regarding the past, present and future in the field of bioceramics. They studied the various advances made in the field of bioactive ceramics, glasses and glass ceramics during the past 30–40 years. They reviewed the ground-breaking work that was performed during the 1970s and 1980s in the field of bioceramics in the production and characterization of bioactive and bioresorbable glasses, glass ceramics and calcium phosphates. In their review they explored the influence of the original concepts and ideas on the more recent development of ceramic scaffolds, composites and coatings with enhanced bioactivity for bone tissue engineering.

First time in the 1920s the similarities between the X-ray diffraction patterns of bone mineral and a calcium phosphate compound, hydroxyapatite was observed. Later Posner *et al.* [16] identified the crystallographic structure of bone mineral and hydroxyapatite. A series of studies in the 1960s, revealed that the presence of carbonate in bone and tooth mineral and hydroxyapatite may be observed directly, using infra-red spectroscopy, in the form of weak peaks between 870 and 880 cm^{-1} and a stronger doublet between 1460 and 1530 cm^{-1} and also through alterations in the hydroxyapatite lattice parameters from X-ray diffraction. The effects of the substitution of electronegative anions, such as fluorine and chlorine for (OH), were also reported to influence the lattice parameters of the structures. However, the main thrust of these studies was characterization and it was not until later in the 1960s and beyond that the development of bioactive ceramics came of age.

It is only in the past 20–30 years that interest in the use of dense hydroxyapatite for implantation has developed and important work was reported in the 1980s and 1990s. The crystal structure of HA can accommodate substitutions by various other ions for the Ca^{2+} PO_4^{3-} and OH^- groups.

The ionic substitutions can affect the lattice parameters, crystal morphology, crystallinity, solubility and thermal stability of HA.

It has been also mentioned in this study that Bonfield *et al.* realised the potential of the use of calcium phosphate as a filler in polymer-matrix composites and the move was envisaged towards improved mechanical performance of HA ceramics. Based on the concept that the structure of bone comprises mineral crystals embedded in a collagen matrix, a method for the twin screw extrusion of composites with a high density polyethylene matrix with homogeneously distributed micron-scale hydroxyapatite particles was developed. The material was successfully developed and marketed under the name HAPEX and used in middle ear implants.

Yusuf *et al.* [17] used the precursors, $Na_2HPO_4.2H_2O$ and $CaCl_2.2H_2O$ for synthesizing pure hydroxyapatite with less carbonate content. The high temperature of sintering, about 700^oC of temperature, was treated to minimize the carbonate group on hydroxyapatite surface. Carbonate content of hydroxyapatite which was sintered in 700^oC was less than 110^oC. It indicated that an increasing temperature of sintering will increase crystallinity and decrease carbonate content of hydroxyapatite. This method gave better way to resulting hydroxyapatite crystal.

The objectives of this research were analyzing the ingredient of carbonate in apatite composite on sintering variation and the effectiveness of hydroxyapatite as a matrix in protein purification. This analysis informed what properties that apatite had if standed as a filter and how apatite can absorb the certain protein and pass through a specific protein.

They concluded from their work that pure hydroxyapatite in less content of carbonate is yielded from wet method preparation in high temperature of sintering that could decrease carbonate content. The sintering temperature which can liberate carbonate depends on how strong polarization of carbonate on hydroxyapatite surface is taken place. To free carbonate on hydroxyapatite is difficult except its preparation was performed in vacuum area without CO_2. The hydroxyapatite is an effective pseudo affinity on protein purification process because the affinity of hydroxyapatite is more than other matrix which can bind a positively and negatively charged protein. Additionally, the use of hydroxyapatite as a matrix is more abiding, it can be used repeatedly more than one hundred times.

Gittings *et al.* [18] studied the ac conductivity and permittivity of hydroxyapatite based ceramics (HA) at temperatures from room temperature to 1000^oC. HA ceramics were prepared either as dense ceramics or in porous form with interconnected porosity and were sintered in either air or

water vapour. Samples were thermally cycled to examine the influence of surface adsorbed water on conductivity and permittivity. Surface bound water was thought to contribute to conductivity for both dense and porous materials at temperature below 200ºC. At temperatures below 700ºC the permittivity and ac conductivity of HA was also influenced by the degree of dehydration and thermal history. At higher temperatures (700-1000ºC), bulk ionic conduction was dominant and activation energies are in the range of ~2eV, indicating that hydroxyl ions are responsible for conductivity.

Bayraktar and Tas [19] prepared the inorganic phase of synthetic bone applications, calcium hydroxyapatite (HA, $Ca_{10}(PO_4)_6(OH)_2$), as a single-phase ceramic powder. Carbonated HA powders were formed from calcium nitrate tetrahydrate and diammonium hydrogen phosphate salts dissolved in aqueous 'simulated body fluid' (SBF) solutions, containing urea (H_2NCONH_2), at 37ºC and pH of 7.4, by using a novel chemical precipitation technique. These powders were also found to contain trace amounts of Na and Mg impurities in them, originated from the use of SBF solutions, instead of pure water, during their synthesis. The characterization and chemical analysis of the synthesized powders were performed by powder X-ray diffraction (XRD), Fourier-transformed infra-red spectroscopy (FT-IR), and inductively-coupled plasma atomic emission spectroscopy (ICP-AES).

They concluded in their study that biological apatites mainly differ from the synthetically produced calcium hydroxyapatites in terms of their carbonate ion content (i.e. the carbonate ion levels being incomparably lower in the latter). Body fluids may be considered as a biomimetic and logical source for increasing the carbonate contents of synthetically prepared HA bioceramics. However, the significantly low levels of HCO^{3-} (i.e. 27mM) in human plasma or SBF solutions makes it impractical for their economically workable use within the shorter 'aging' times allowed in powder synthesis technology, as compared to the aging of natural bones offsprings in the human body for a typical period of `9 months and 10 days'. The as-filtered/dried calcium phosphate precipitates formed at 37ºC and pH of 7.4 via 'pure SBF' (i.e. without urea) solutions were found to be amorphous. Upon calcination of these amorphous powders, in a stagnant air atmosphere, at 1100ºC for 6 hrs, they completely transformed into crystalline, single-phase HA. The HA precipitates of this study formed in 'pure SBF' solutions, uncommonly, had an excellent thermal stability even when heated at 1600ºC for 6 h in an air atmosphere.

Darimont *et al.* [20] did some research work to evaluate quantitatively the behaviour of in vivo hydroxyapatite coated implants (HA) in the rabbit over time, and to compare the results with observations made on titanium plasma spray implants (TPS). They analysed their results according to the percentage of bone contact. So the aim of this study was to investigate the physical changes of an HA coating on a titanium substrate. They compared it with TPS coated implants placed in rabbit femur epiphysis. Evaluation of histomorphometrical data demonstrated a good HA coating stability, principally in cortical bone, where a close bone contact was observed. In contrast, a significant decrease of HA thickness was observed in the marrow area, where the lowest bone-to-implant contact was reported. These findings confirmed earlier observations. Authors described a poor bone contact between the HA coating of a total hip prothese and marrow of the human femur. Others observed a higher resorption rate of the HA thickness in bone marrow in contrast with cortical or trabecular bone.

In the case of TPS coatings, neither the amount of bone contact nor the implantation period modified the thickness of the coating. The different measurements showed that a more complete bone contact preserves the HA coating, thus this indicates that bone protected the HA coating from degradation adjacent to cortical bone. Also, light microscopic evaluations revealed that bone formation proceeded faster and resulted in more bone apposition for HA implants than for TPS implants. In general calcium-phosphate coatings, whatever their composition, promote bone apposition and differentiation of mesenchymal cells to osteoblasts, however, the exact role of these ceramics on bone healing is still unknown.

Webster *et al.* [21] performed a study to analyze about the fact that nanocrystalline hydroxyapatite enhances osteoblast function. They reported that osteoblast (boneforming cells) adhesion, proliferation and formation of calcium-containing mineral deposits is enhanced on ceramics (such as alumina and titania) of grain sizes less than 100 nm. Conventional hydroxyapatite (HA), the major inorganic constituent of physiological bone, has been shown to enhance osteoblast function. The present *in vitro* study, the first of its kind, investigated osteoblast function (specifically, adhesion and proliferation) on nanocrystalliine (that is, grain sizes less than 100 nm) HA.

Crystalline HA ($Ca_5(PO_4)_3OH$) was prepared via established wet chemistry synthesis. Briefly, over a five minute interval, calcium nitrate was added to ammonium hydroxide: water solution and stirred for 24 hours; HA precipitates were formed during this time period and grain size was

controlled by stirring the calcium nitrate ammonium hydroxide: water solution at either room temperature for 24 hours (for 50 nm grain size HA) or at 90ºC for 1 and 3 hours (for 150 and 250 nm grain size HA, respectively). The HA containing solution was then centrifuged, filtered, dried, and sintered (in air at 10ºC/minute) at 1100°C for 60 minutes. HA grain size and topography was determined by scanning electron microscopy; crystallinity of HA was determined by X-ray diffraction.

They have reported that osteoblast adhesion as well as proliferation were significantly ($p < 0.01$) greater on nanocystalline (50 nm grain size) than on conventional (250 nm grain size) HA at all time periods tested. Since enhanced osteoblast function undoubtedly contributes to greater biomaterial bonding to juxtaposed bone (an event that will aid in the clinical success of orthopaedic/dental implants), the improved cytocompatability properties of nanocystalline HA should be considered when designing biomaterials of the future.

Eslami *et al.* [22] synthesized hydroxyapatite nanocrystals via chemical precipitation technique by using diammonium hydrogen phosphate and calcium nitrate 4-hydrate as starting materials and sodium hydroxide solution was used as the agent for pH adjustment. They evaluated the powder sample by techniques such as scanning electron microscope, transmission electron microscope, Fourier transform infra-red spectroscopy, differential thermal analysis, thermal gravimetric analysis, X-ray diffraction, atomic absorption spectroscopy and EDTA titration analyses. Andto from their experimental results, they found that hydroxyapatite nanocrystals can be successfully produced through wet precipitation method. The bulk Ca/P molar ratio of synthesized hydroxyapatite was determined as 1.71 that was higher than stoichiometric ratio (1.667) which is expected for a pure HA phase. Finally, transmission electron microscopic technique confirmed that the crystallites of prepared powder were nanosized with a needle-like morphology.

Tong *et al.* [23] studied about post-treatment of plasma sprayed hydroxyapatite coatings with water vapour. They revealed that it is important to transform the amorphous and the additional phases, such as α, β-$Ca_3(PO_4)_2$, (α, β-TCP) and $Ca_4O(PO_4)_2$ (TP), into HA and thus increase crystallinity of the coatings in terms of long-term stability. Post-treatment is an effective way to increase crystallinity of the coating which includes water vapour treatment with water vapour pressure of 0.15 MPa and post-heat-treatment in different atmosphere. They found that TCP and TP disappeared almost completely after water vapour treatment but the amorphous to crystalline

conversion was still incomplete. Post-heat-treatment at 490ºC in air with water vapour can obtain a completely crystalline HA coating after 2h treatment, which is superior to both water vapour treatment and post-heat-treatment in air without water vapour in terms of phase transition. Amorphous to crystalline conversion is significantly promoted when temperature and water vapour pressure increased whereas increase in water pressure or temperature alone is not efficient in this conversion. They concluded in their study that effect of water vapour on the amorphous to crystalline conversion is insufficient if the temperature is low, but it is significant when temperature is increased to certain critical point.

Xin *et al.* [24] investigated the formation of calcium phosphate (Ca-P) on various bioceramic surfaces in SBF and in rabbit muscle sites. The bioceramics were sintered porous solids, including bioglass, glass-ceramics, hydroxyapatite, α-tricalcium phosphate and β-tricalcium phosphate. The ability of inducing Ca-P formation was compared among the bioceramics. The Ca-P crystal structures were identified using single-crystal diffraction patterns in transmission electron microscopy. The examination results showed that ability of inducing Ca-P formation in SBF was similar among bioceramics, but was considerably different among bioceramics *in vivo.* Sintered β-tricalcium phosphate exhibited a poor ability of inducing Ca-P formation both *in vitro* and *in vivo.* Octacalcium phosphate (OCP) was formed on the surfaces of bioglass, A-W, hydroxyapatite and α-tricalcium phosphate *in vitro* and *in vivo.*

Kon *et al.* [25] studied a functional gradient bioceramic that can function gradually with respect to body tissue by changing the composition of calcium phosphate gradually from the surface to the inside. Diamond powder was spread on the surface of compact hydroxyapatite (HA) powder and fired at 1280°C under reduced pressure, followed by firing under atmospheric conditions. The sintered body thus prepared was dense and α-tricalcium phosphate (α-TCP: α-$Ca_3(P0_4)_2$ was found on its surface. The content of α-TCP gradually decreased with increasing depth from the surface. In contrast, the content of HA increased with increasing depth from the surface. The gradient ratio of α-TCP and HA depends on the firing time for each condition, i.e. reduced or atmospheric pressure. This functional gradient bioceramic consisting of HA and α-TCP showed potential value as bone-replacing or bone-substituting materials since α-TCP gradually decreased from the surface to the interior.

CHAPTER 3

EXPERIMENTAL DETAILS

3.1 Introduction

In this chapter, the design and working of experimental setup used for preparation and characterization of hydroxyapatite have been described. In addition, the detailed sample preparation procedure and procedure employed for X- ray diffraction (XRD), Scanning Electron Microscopy (SEM) and weight loss measurements by Thermogravimetric Analysis (TGA) are given in details.

3.2 Sample Preparation

Several methods have been utilized for the synthesis of HAP, which includes precipitation technique, sol-gel method, hydrothermal technique, multiple emulsion technique, biomimetic deposition technique, electrodeposition technique etc.

In present study the sol-gel method as suggested by Agrawal *et al.* [26] has been used to prepare hydroxyapatite powder (HA) and HA-CNT composite. The following materials were used as raw materials or starting materials.

1. Phosphoric pentoxide P_2O_5; molecular weight → 141.94 g/mol
2. Calcium nitrate tetrahydrate $Ca(NO_3)_2.4H_2O$; molecular weight → 236.15 g/mol

At first phosphoric pentoxide (P_2O_5) is dissolved in absolute ethanol to form a 0.5 mol/litre solution and secondly calcium nitrate tetrahydrate ($Ca(NO_3)_2.4H_2O$) is also dissolved in ethanol to form 1.67 mol/litre solution. After this, both the solutions are mixed to obtain the desired Ca/P molar ratio of 1.67.

The whole procedure of preparing the HA powder is as shown in the following flow diagram (Figure 3.1).

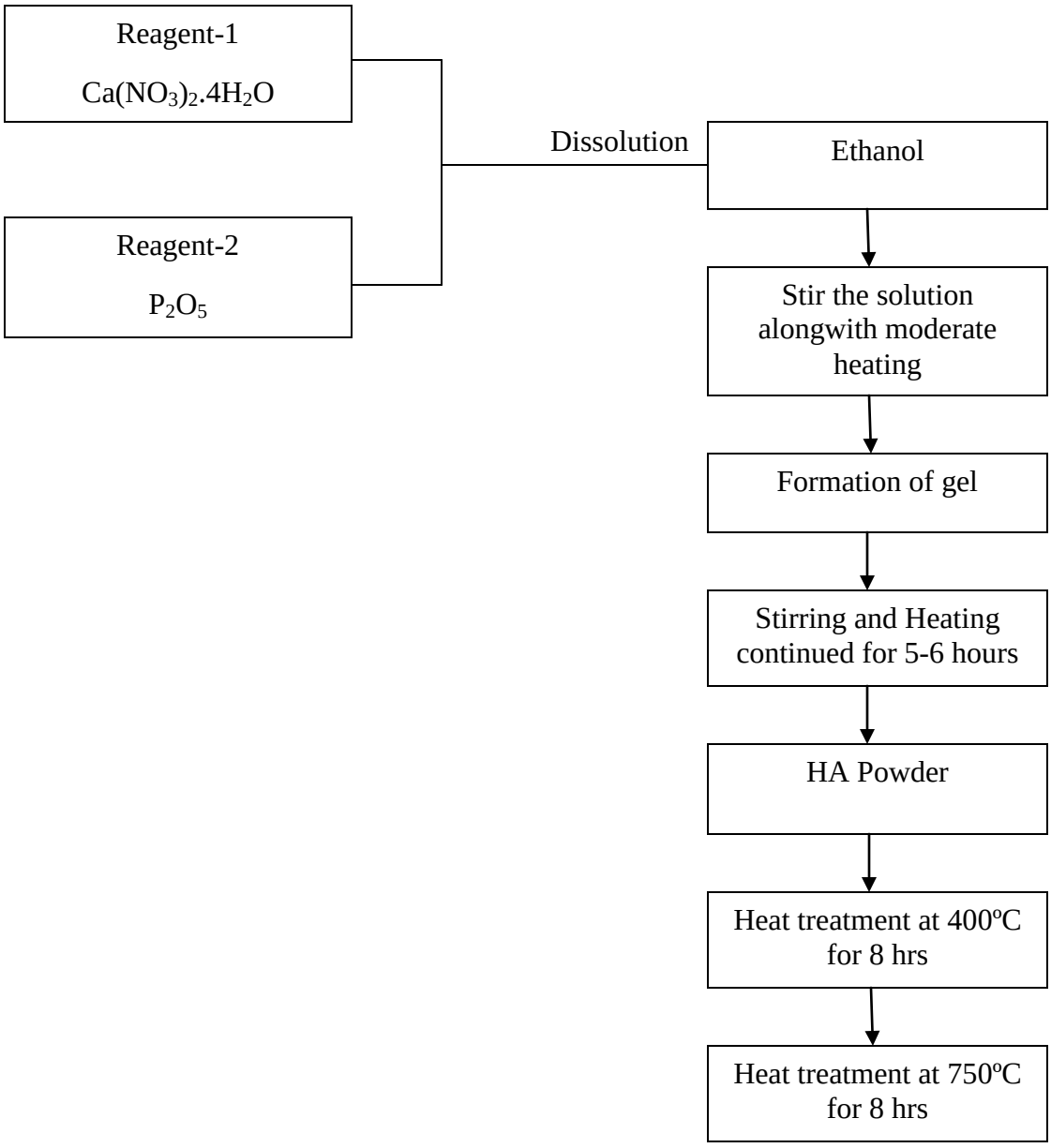

Figure 3.1 Schematic flow process chart for the synthesis of HA powder by the use of $Ca(NO_3)_2.4H_2O$ and P_2O_5

For making the solution of 1mol/litre concentration of $Ca(NO_3)_2.4H_2O$ we need 236.15 g of calcium nitrate tetrahydrate in 1 litre ethanol as according to the molecular weight of $Ca(NO_3)_2.4H_2O$, one mol is equivalent to 236.15 g. Correspondingly for making 1.67 mol/litre solution we need 394.37 g of calcium nitrate tetrahydrate in one litre of ethanol. In the same way we need 70.97 g of phosphoric pentoxide in one litre of ethanol to form 0.5 mol/litre solution.

The sample was prepared by dissolving both the chemicals into 50 ml ethanol. So accordingly the required amount of the chemicals were calculated which appeared to be as follows:

- Calcium nitrate tetrahydrate ($Ca(NO_3)_2.4H_2O$) →19.72 g in 50 ml ethanol.
- Phosphoric pentoxide (P_2O_5) → 3.54 g in 50 ml ethanol.

1. First of all the calculated amount of calcium nitrate tetrahydrate and phosphoric pentoxide were dissolved in 50 ml ethanol each in two separate 100 ml beakers. Then both the solutions were mixed together gradually into a 250 ml beaker.

2. After that the solution was stirred by using magnetic stirring needle for 15-20 minutes.

3. Then heating was also started along with stirring and the temperature was kept around 70ºC.

4. So during stirring and heating the gel was formed after near about 2 hours and after 6-7 hours the powder was formed in a dry condition.

5. This powder was taken out of the beaker and grinded for homogeneous distribution of particles throughout the powder.

6. Further this powder was sintered at 400ºC and 750ºC for 8 hours separately.

The chemical reaction occurred during the above process is as given below:

$$10\ Ca(NO_3)_2.4H_2O + 3\ P_2O_5 \rightarrow Ca_{10}(PO_4)_6(OH)_2 + 20\ HNO_3 + 29\ H_2O \qquad (1)$$

The nitric acid and water are the byproducts of the reaction.

Some samples of HA powder obtained in first step *i.e.* without any sintering were also washed with distilled water by using laboratory bench-top centrifuge. The sample was washed three times and time for each washing given in the centrifuge was 10 minutes at 3400 rpm. A significant part of the powder used for washing was lost during the washing process. For illustration, 8.51 g powder was used for washing and 6.96 g powder was lost during the washing and only 1.55 g powder was obtained after washing and drying it. So it was observed that almost 82% powder has been lost in the washing process.

Another sample was prepared by embedding the CNTs into the powder *i.e.* HA-CNT composite. CNTs were embedded just 15-20 after the stirring was started and rest of the procedure was same as mentioned above. CNTs were in powder form and 20 mg CNTs were mixed into the solution of the earlier mentioned calculations. Figure 3.2 shows the schematic flow process chart for the synthesis of HA-CNT composite by the use of $Ca(NO_3)_2.4H_2O$ and P_2O_5.

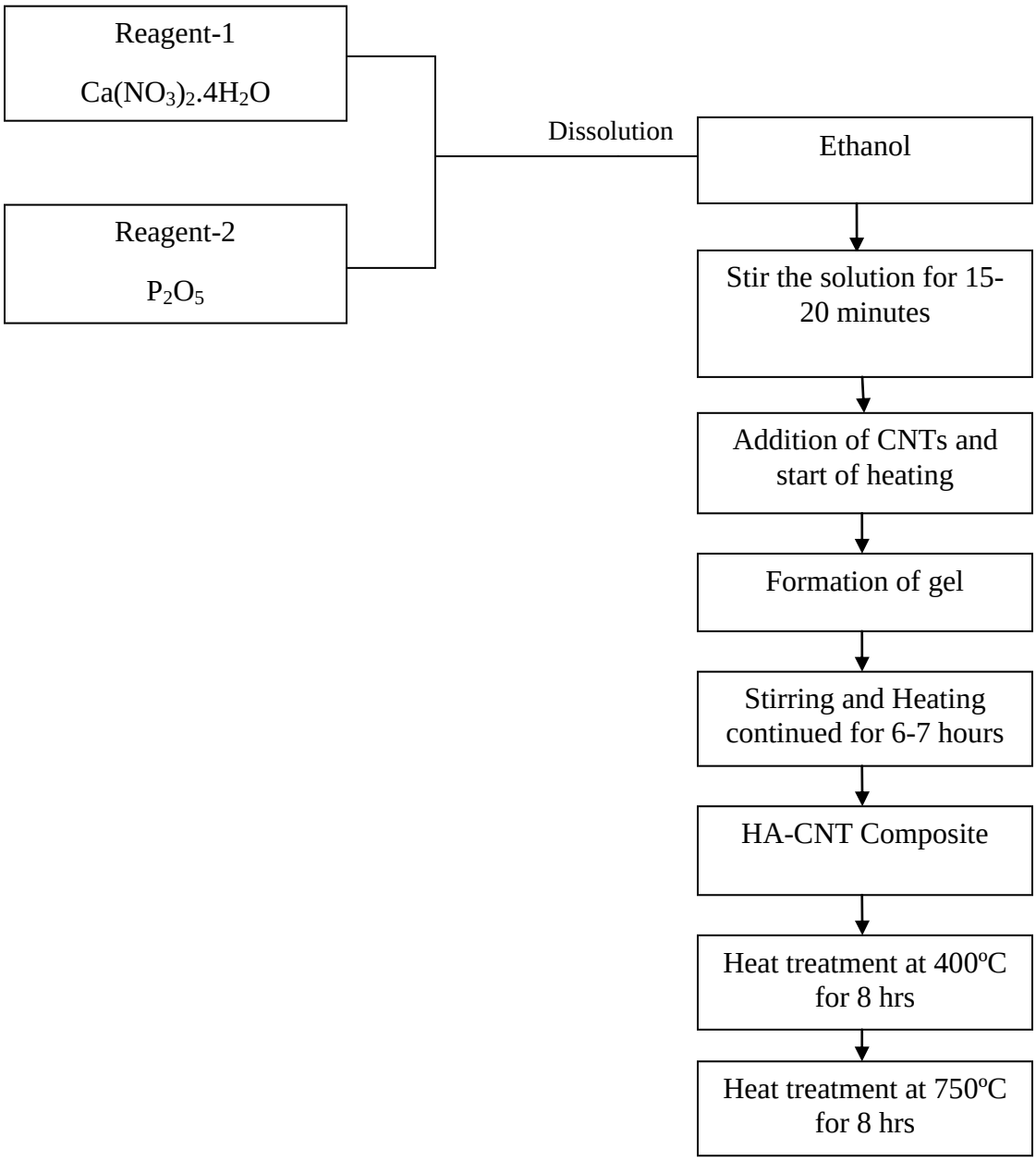

Figure 3.2

3.3 Details and Labels of Various Samples

Sample 1 HA powder sample without any heat treatment and washing

Sample 2 HA powder sample washed and sintered at 400ºC for 8 hours

Sample 3 HA powder sample washed and sintered at 750ºC for 8 hours

Sample 4 HA-CNT composite powder sample washed and sintered at 750ºC for 8 hours

3.4 X-ray diffraction (XRD)

In order to confirm the crystalline nature of the HA sample & to find the change in its crystallinity after sintering, X-ray diffraction study had been made on HA samples using Cu Kα radiation (λ = 1.5418 Å). X-ray Diffraction (XRD) is a powerful non-destructive technique for characterizing crystalline materials. It provides information related to structures, phases, preferred crystal orientations, and other structural parameters, such as crystallinity, strain. X-ray diffraction peaks are produced by constructive interference of monochromatic beam of x-rays scattered at specific angles from each set of lattice planes in a sample. The phenomenon is called X-ray diffraction. The X-ray diffraction follows the Bragg's law as follows.

$$2\,d \sin\theta = n\lambda$$

Where λ is the wavelength of incident X-ray, d is the interplanar distance and θ is diffraction angle.

3.5 Thermogravimetric Analysis (TGA)

Thermogravimetric analysis (TGA) is the most widely used thermal analysis method. It is based on the measurement of mass loss of material as a function of temperature. In thermogravimetry a continuous graph of mass change against temperature is obtained when a substance is heated at a uniform rate or kept at constant temperature. A plot of mass change versus temperature (T) is referred to as the thermogravimetric curve (TG curve). TG curve helps in revealing the extent of purity of analytical samples and in determining the mode of their transformations within specified range of temperature [27].

Thermogravimetric analysis can be used for the following analysis:

- Purity and thermal stability
- Solid state reactions
- Decomposition of inorganic and organic compounds
- Determining composition of the mixture
- Corrosion of metals in various atmospheres
- Roasting and calcinations of minerals
- Reaction kinetics studies
- Oxidative and reductive stability
- Determining moisture, volatile and ash contents

In present study the Thermal analysis of the samples has been done by heating up to 1200ºC at a heating rate of 5ºC/minute to check the weight loss and thermal stability of the powder.

3.6 Scanning Electron Microscopy (SEM)

The scanning electron microscope (SEM) uses a focused beam of high-energy electrons to generate a variety of signals at the surface of solid specimens. The signals that develop from electron-sample interactions reveal information about the sample including external morphology (texture), chemical composition, and orientation of materials making up the sample. In most applications, data are collected over a selected area of the surface of the sample, and a 2-dimensional image is generated that displays spatial variations in these properties. The analyses of selected point locations can also be done on the sample; this approach is especially useful in qualitatively or semi-quantitatively determining chemical compositions (using EDS) [28].

Accelerated electrons in an SEM carry significant amounts of kinetic energy, and this energy is dissipated as a variety of signals produced by electron-sample interactions when the incident electrons are decelerated in the solid sample [28].

Figure 3.3 Set up of SEM Instrument

These signals include secondary electrons (that produce SEM images), backscattered electrons (BSE), photons (characteristic X-rays that are used for elemental analysis and continuum X-rays), visible light (cathode luminescence--CL), and heat. Secondary electrons and backscattered electrons are commonly used for imaging samples: secondary electrons are most valuable for showing morphology and topography on samples and backscattered electrons are most valuable for illustrating contrasts in composition in multiphase samples (i.e. for rapid phase discrimination [28].

CHAPTER 4

RESULTS AND DISCUSSION

4.1 X-ray diffraction analysis

Figure 4.1 shows the typical X-ray diffraction pattern of the HA powder washed and sintered at 400°C for 8 hours. The X-ray pattern of this sample possessed the characteristic hump. This hump in the XRD pattern reveals the "amorphous" nature of the sample. Ungureanu *et al.* [29] have reported that the nano powder of hydroxyapatite converted into crystalline phase above 200°C. The crystallinity increases with increasing heating temperature.

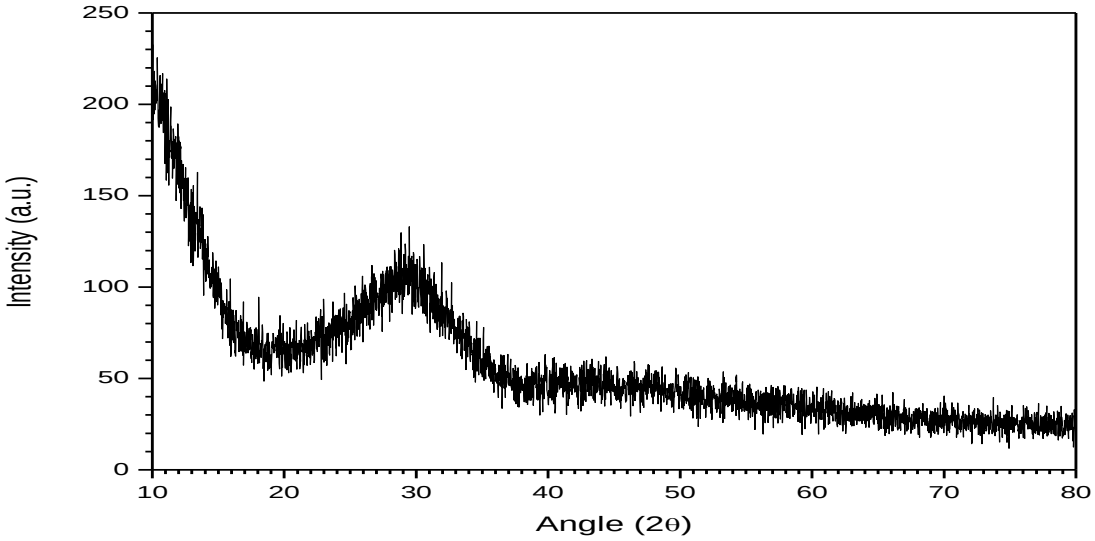

Figure 4.1 XRD pattern of the sample 2.

Figure 4.2 shows the XRD pattern of sample 3, washed and sintered at 750°C for 8 hours. Similarly, the XRD pattern of sample 4 *i.e.* the HA-CNT composite powder washed and sintered at 750°C for 8 hours is also shown in figure 4.2. For sample 3 the peaks positioned at 31.63°, 29.72° and 27.80° were indexed to (221), (-132) and (-112) crystal planes, respectively. These three peaks and the other peaks marked as '+' are indexed to the hydroxyapatite, (ICDD card No. 01-089-4405). It is the main phase formed with the monoclinic crystal lattice. The volume fraction of hydroxyapatite was observed to be 68% in sample 3 as marked as phase A.

Except the HA powder, calcium phosphate hydrate was also present in the powder as shown in figure 4.2. The secondary phase has been indexed to calcium phosphate hydrate (ICDD card No. 01-070-4788). This phase has been represented as phase B and the volume fraction of this phase is found 32%.

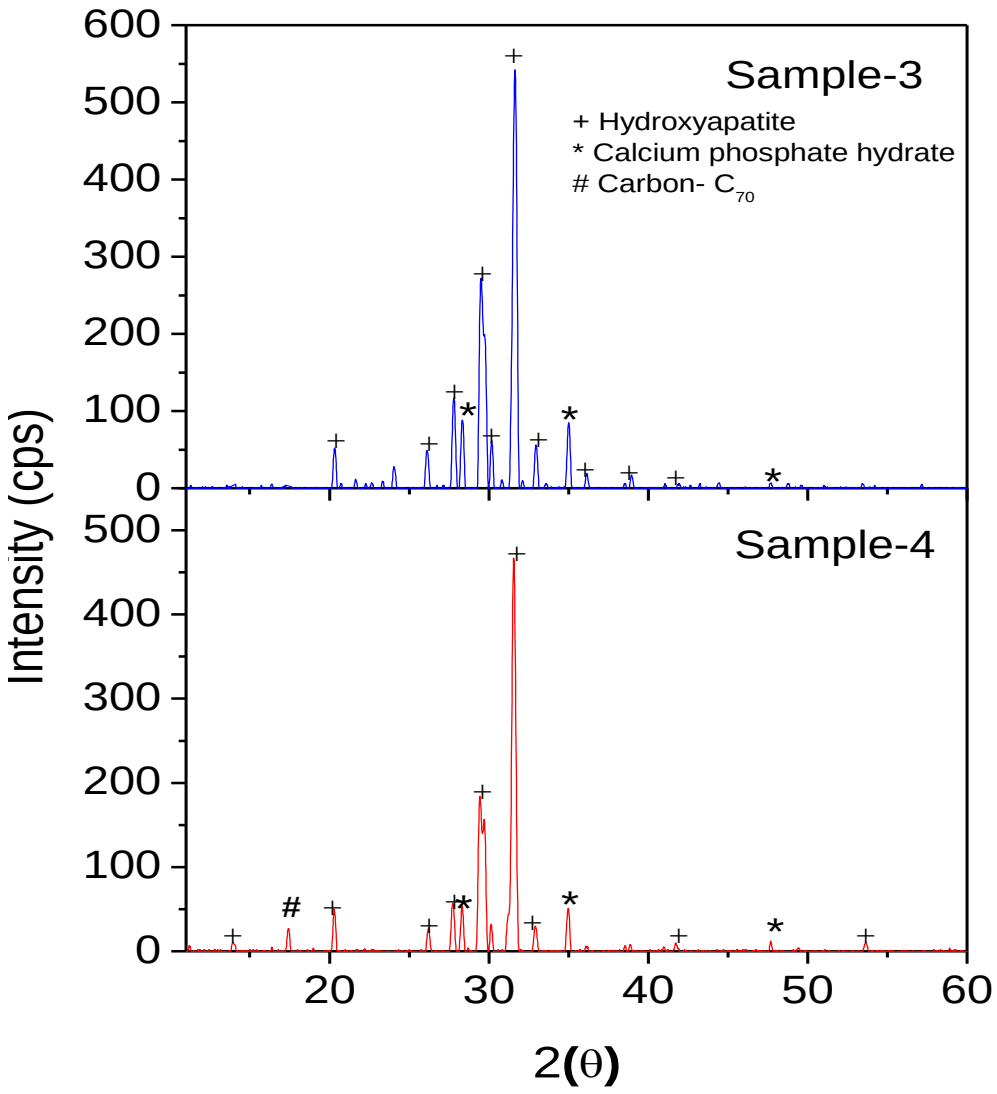

Figure 4.2 XRD pattern of the sample 3 and 4.

As compared to Sample 3, the addition of CNTs in sample 4 leads to the shifting of XRD peaks towards lower diffraction angle which indicates the presence of some tensile stress in the sample.

It may be attributed due to occupation of interstitial sites in the lattice of HA phase by carbon. The following table 4.1 describes the diffraction angle according to peaks observed, phase present and crystal plane for each peak for sample 3.

Table 4.1 Diffraction data for sample 3.

2θ (degrees)	**Phase**	**(hkl)**
13.93	A	(011)
20.31	A	(031)
26.10	A	(012)
27.80	A	(-112)
28.31	B	(220)
29.72	A	(-132)
30.17	A	(051)
31.63	A	(221)
32.94	A	(060)
34.99	B	(-223)
41.91	A	(161)
47.69	A	(133)
53.42	A	(-114)

For sample 4 the peaks positioned at 31.54°, 29.71° and 27.72° were indexed to (221), (-132) and (-112) crystal planes, respectively. These peaks and the other peaks marked as '+' in the pattern are indexed to the hydroxyapatite powder as per ICDD card No. 01-089-4405. Like in sample 3, in this sample also, it is main phase with 67% volume fraction of this phase and denoted as phase A. The other phase present, as secondary phase, was calcium phosphate hydrate. The secondary phase has been indexed to calcium phosphate hydrate (ICDD card No. 01-070-4788). The volume fraction of this phase is 31% in the concerned sample. Furthermore, due to addition of CNTs, some traces of carbon were also seen in the XRD pattern as shown by the marked peak positioned at 17.42° in the XRD pattern of sample 4. Carbon has been designated as phase C and its volume fraction is about 2%.

Table 4.2 Diffraction data for sample 4.

2θ (degrees)	Phase	(hkl)
13.93	A	(011)
17.42	C	(130)
20.29	A	(031)
26.20	A	(012)
27.72	A	(-112)
28.31	B	(220)
29.71	A	(-132)
30.15	A	(051)
31.54	A	(221)
32.90	A	(060)
34.96	B	(-223)
41.71	A	(161)
47.68	B	(133)
53.61	A	(-114)

The XRD patterns were also used to calculate the crystallite size of both the samples using classical Scherrer equation.

$$D = \frac{0.9\,\lambda}{\beta cos\theta} \quad \ldots (1)$$

Where D is crystallite size, λ is wave length of incident x-ray, β is Full Width at Half Maximum (FWHM) and θ is the half of the diffraction angle of the corresponding peak. The comparison between crystallite size of sample 3 and 4 has been shown in table 4.3. The crystallite size is around 31 nm for sample 3. On the other hand, sample 4 exhibits larger crystallite size *i.e.* around 36 nm. It is also evident from XRD pattern as peaks are sharper in sample 4 than sample 3. The addition of CNTs enhance the crystallinity as crystallite size changes from 31 nm to 36 nm. The crystallite size of HA phase is more or less similar order as reported by Ungureanu *et.al.* [29] for HA phase which was synthesized by chemical precipitation method.

Table 4.3 Crystallite size of sample 3 and 4.

	Sample 3	**Sample 4**
λ (Å)	1.54	1.54
FWHM (radians)	4.595×10^{-3}	4.054×10^{-3}
θ (radians)	0.2764	0.2754
Cosθ	0.9620	0.0.962
Average Crystallite size (nm)	31	36

4.2 Thermal analysis (TGA-DTA)

The TGA curve of as prepared sample *i.e.* sample 1 is shown in figure 4.3. The sample has not been given any heat treatment before the TGA analysis. The TG curve could not show sharp defined steps as reported by Hui *et.al.* [30]. The pattern shows that there is weight loss of about 20% up to 70°C which may be mainly due to loss of absorbed water content and approximately 30% weight loss has been observed in the temperature range of 70°C to 350°C. Further, about 6% weight loss was observed in the range of 350°C to 500°C. Beyond 500°C to 1000°C no significant weight loss was observed. Almost stable curve was observed in this temperature range.

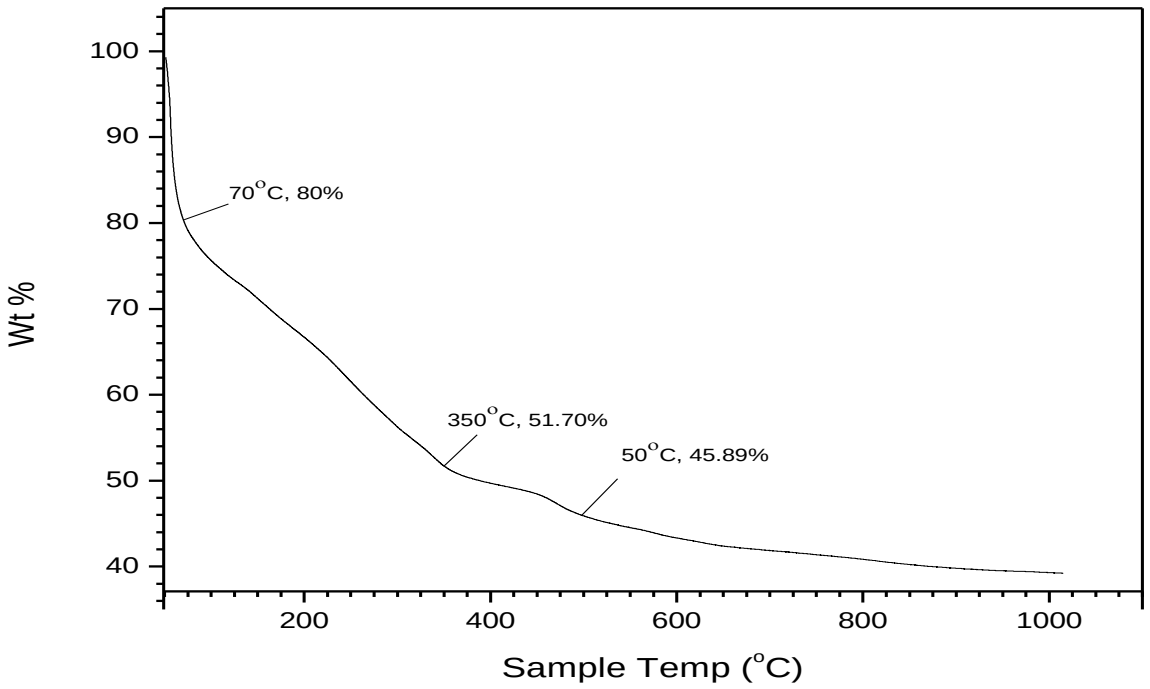

Figure 4.3 TGA pattern of the sample 1.

The heat treated and CNT added sample shows better thermal stability as compared to as prepared sample as shown in figure 4.4. TGA analysis shows that there is weight loss of about 0.5% up to temperature 200°C. This loss is mainly due to loss of the absorbed water content. Further another weight loss of about 1.54% has been observed in the temperature range of 240°C to 600°C. This weight loss may be due to evaporation of some volatile substances present in the powder. This weight loss can be seen as the result of increased crystallinity of the powder. Further, beyond 600°C, the powder showed a continuous weight loss with respect to temperature which is mainly due to the carbon loss from the powder which was present because of embedding of CNTs in to the sample. This continuous decrease in the weight indicates that the prepared powder does not possess thermal stability.

In comparison to as prepared sample TGA, the sample 4 curve shows better stability. The less slope becomes more clear. The heat treated sample is melted at 1150°C as observed in figure 4.4.

The melting point of HA is 1100°C. It is reported in the same range as observed in the present sample.

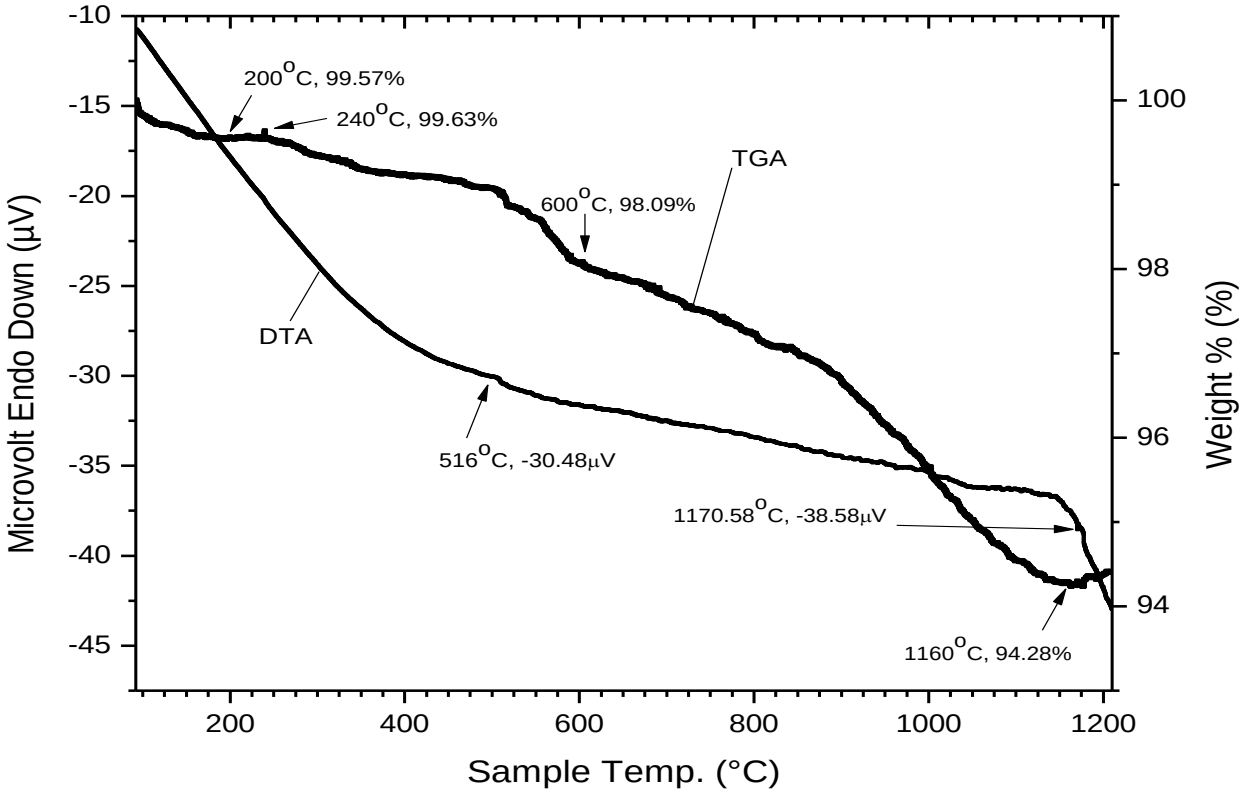

Figure 4.4 TGA-DTA pattern of the sample 4.

The DTA curve of this sample shows a broad exothermic peak started at ~1150°C. It might belong to the melting of HA layer.

4.3 SEM and EDS Analysis

Figure 4.5 shows the SEM image of sample 3 which was sintered at 750°C for 8 hours. These images were taken in secondary emission mode. The image reveals the formation of HA powder made up of agglomeration of nano sized grains. The grains may be agglomerated due to the formation of gel during the synthesis process.

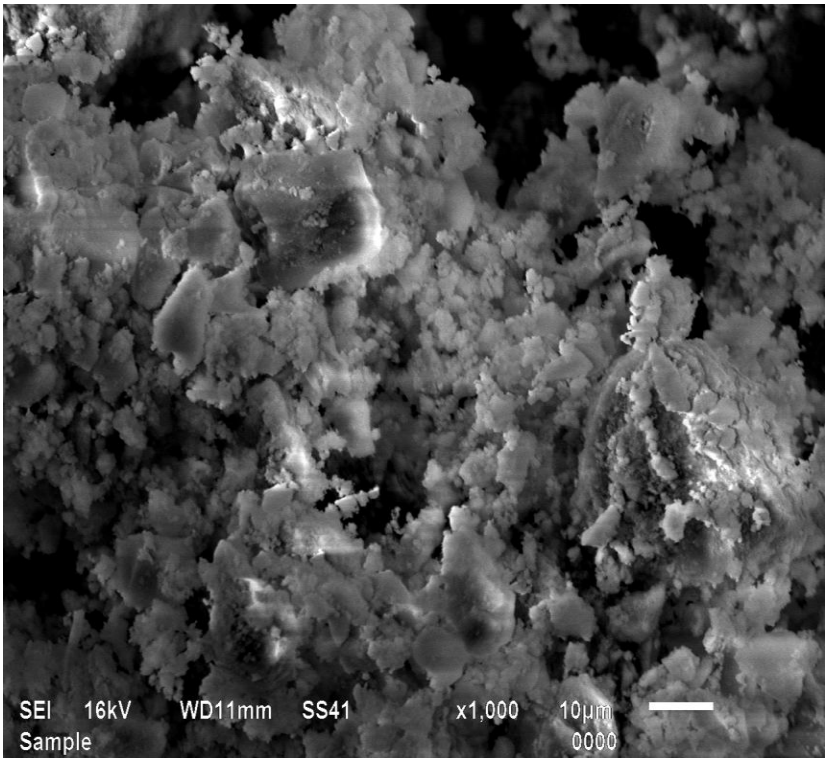

Figure 4.5 SEM micrograph of sample 3.

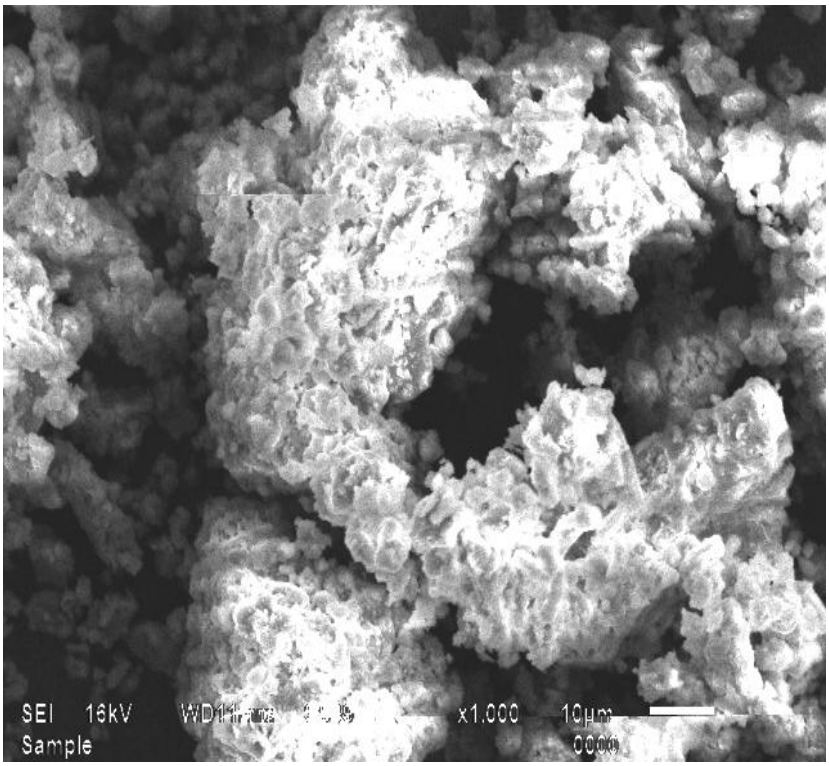

Figure 4.6 SEM micrograph of sample 4.

Figure 4.6 shows the SEM image of sample 4 *i.e.* HA-CNT composite which was sintered at 750°C for 8 hours. Due to agglomeration, it is very difficult to estimate the particle size. The shapes of the particles are either spherical or semispherical. The agglomeration tendency is more pronounced in sample 4 as compared to sample 3 as shown in figure 4.5 and 4.6. Moreover, the agglomeration of the crystallites leaves bigger pores as observed in these figures. Sometimes, the porosity in biomaterials is beneficial to permit the circulation of body fluid when it is used as implants [12].

The EDS was also performed on the sample 3 and sample 4 to check the weight percentage of different elements present in these samples. The theoretical weight percentage of various elements present in the powder was calculated with the help of XRD pattern of the samples and the practical weight percentage was observed from EDS spectrum of the samples. These two values were compared with each other.

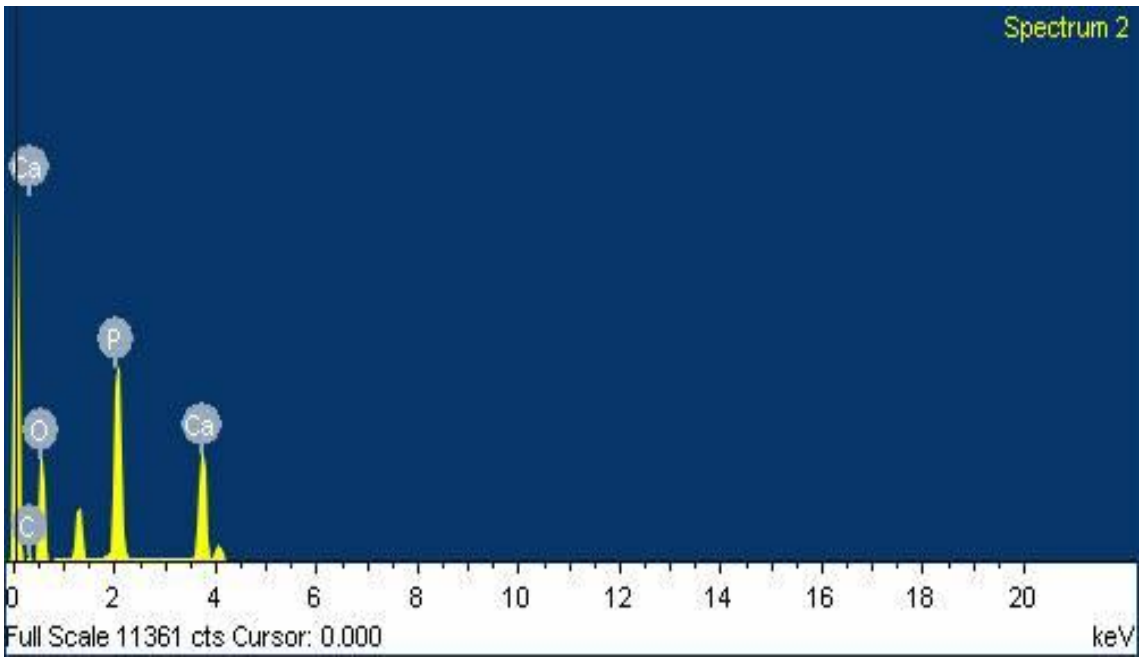

Figure 4.7 EDS spectrum of sample 3.

Figure 4.7 shows the EDS spectrum of sample 3 which was sintered at 750°C for 8 hours. Some carbon content had been observed which may be present due to grid beneath the sample.

Table 4.4 shows the comparison between theoretical and practical weight percentage of elements in sample 3.

Table 4.4 Elemental weight percentage comparison for sample 3.

Element	Theoretical Weight %age	Experimental Weight %age
Ca	36.31	19.01
P	19.34	21.51
O	44.35	59.48

Figure 4.8 shows the EDS spectrum of sample 4 *i.e.* HA-CNT composite which was sintered at 750°C for 8 hours. Table 4.5 shows the comparison between theoretical and experimental weight percentage of elements in sample 4. The EDS analysis clearly indicates the presence of Ca, P, O and C, which are present in hydroxyapatite phase.

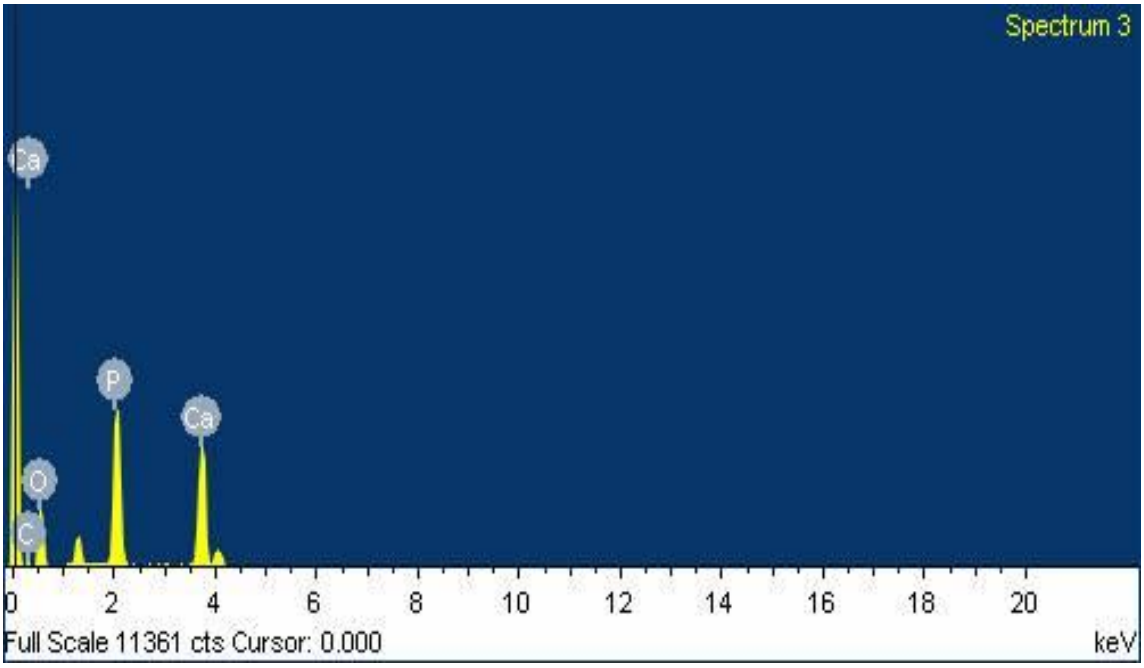

Figure 4.8 EDS spectrum of sample 4.

Table 4.5 Elemental weight percentage comparison for sample 4.

Element	Theoretical Weight %age	Experimental Weight %age
Ca	35	23.10
P	17.92	19.79
O	42.66	50.72
C	4.42	6.39

CHAPTER 5

CONCLUSION AND FUTURE SCOPE

In the present study, the samples are prepared by sol-gel technique. The as prepared samples show the amorphous nature. The higher temperature heat treatment (750°C/8 hours) leads to the formation of HA and hydrate phase. The volume fraction of these phases is 67% and 31% respectively. The addition of CNTs, in as prepared and heat treated samples, increased the crystallinity and thermal stability along with crystallite size. The SEM study clearly shows the agglomeration with higher porosity. The melting point is observed ~1150°C. EDS analysis clearly shows the presence of hydroxyapatite and related phase. However, these phases are chemically non-stoichiometric as calculated from the weight percentage of different elements.

Fourier Infrared spectroscopy measurement could be performed to confirm the formation of HA phase. Furthermore, characterization such as TEM is required to confirm the particle size. The nano sized HA powder formed can be highly useful as a bone implant.

References

1. A. Tathe, M. Ghodke and A. P. Nikalje, International Journal of Pharmacy and Pharmaceutical Sciences 2 (2010), 19-23.
2. E. Sahin, Synthesis and Characterization of Hydroxyapatite-Alumina-Zirconia Biocomposites, Graduate School of Engineering and Sciences of Izmir Institute of Technology, (2006).
3. http://media.wiley.com/product_data/excerpt/44/04712539/0471253944.pdf
4. T. J. Blokhuis, M. F. Termaat, F. C. den Boer, P. Patka, F. C. Bakker, and H. J. Th. M. Haarman. The Journal of Trauma: Injury, Infection, and Critical Care 48 (2000), 179-186.
5. http://www.azom.com/article.aspx?ArticleID=2630
6. G. Maccauro, P. R. Iommetti, L. Raffaelli and P. F. Manicone, Biomaterials Applications for Nanomedicine, Rosario Pignatello (Ed.) (2011).
7. T. V. Thamaraiselvi and S. Rajeswari, Trends Biomater. Artif. Organs 18 (1) (2004) 9-17.
8. W. Cao & L. L. Hench, "Bioactive Materials", Ceramics International 22 (1996), 493-507.
9. L. L. Hench, J.Am. Ceram. Soc. 74 (7) (1991) 1487-1510.
10. A. A. White and S. M. Best, International Journal of Applied Ceramic Technology 4(1) (2007), 1-13.
11. D.Zhang, Academic Dissertation, In vitro Characterization of Bioactive Glass by, Åbo Akademi University, Faculty of Technology, Laboratory of Inorganic Chemistry (2008), ISSN- 1459- 18205.
12. S. V. Dorozhkin, J. Funct. Biomater. 1 (2010), 22-107.
13. T. Kokubo, Biocreamics and their clinical applications, JMM, Woodhead Publishing Limited (2008).
14. http://www.azom.com/article.aspx?ArticleID=107
15. S.M. Best, A.E. Porter, E.S. Thian , J. Huang, Journal of the European Ceramic Society 28 (2008), 1319–1327.

16. A. S. Posner, A. Perloff, and A. F. Dionio, Acta Cryst 11 (1958), 308–309.

17. P. Sari, M. Yusuf, K. Dahlan, and A. B. Witarto, Makara, sains 13(2) (2009)134-140.

18. J.P. Gittings, C.R. Bowen, I.G. Turner, A.C.E. Dent, F.R. Baxter and J.B. Chaudhuri, Whittles Publishing Ltd. (2008),

19. D. Bayraktar and A. CuÈ neyt Tas, Journal of the European Ceramic Society 19 (1999), 2573-2579.

20. G.L. Darimont, R. Cloots, E. Heinen, L. Seidel, R. Legrand, Biomaterials 23 (2002), 2569–2575.

21. T. J. Webster, C. Ergun, R. H. Doremus, R. W. Siegel, and R. Bizios, Proceedings of The First Joint BMES/EMES Conference Serving Humanity, Advancing Technology Oct. 13-16(1999), Atlanta, GA, USA.

22. H. Eslami, M. S. Hashjin, M. Tahriri, Iranian Journal of Pharmaceutical Sciences Spring 4(2) (2008), 127-134.

23. W. Tong, J. Chen, Jiaming Feng, Yang Cao, Lin Lu and Xingdong Zhang 0-7803-3131-1 (1996), 160-163.

24. R. Xin, Y. Leng, J. Chen, Q. Zhang, Biomaterials 26 (2005), 6477–6486.

25. M. Kon, K. Ishikawa, Y. Miyamoto and K. Asaoka, Biomaterials 16 (1995), 709-714.

26. K. Agrawal, G. Singh, D. Puri, S. Prakash, Journal of Minerals & Materials Characterization & Engineering, 10(8) (2011), 727-734.

27. http://vedyadhara.ignou.ac.in/wiki/images/1/1c/UNIT_10_THERMOGRAVIMETRIC_ANALYSIS.pdf

28. http://serc.carleton.edu/research_education/geochemsheets/techniques/SEM.html.

29. D. N. Ungureanu, N. Angelescu, R. M. Ion, E. V. Stoian, C. Z. Rizescu, Recent Researches in Communications, Automation, Signal Processing, Nanotechnology, Astronomy and Nuclear Physics (Published in proceeding) (2011), 296-391.

30. P. Hui, S.L. Meena, G. Singh, R.D. Agarawal, S. Prakash, Journal of Minerals & Materials Characterization & Engineering, 9 (8) (2010), 683-692.